

# Non-equilibrium correlations in minimal dynamical models of polymer copying

Jenny M Poulton and Thomas E Ouldridge

*Department of Bioengineering, Imperial College London, London SW7 2AZ, United Kingdom*

Pieter Rein ten Wolde

*FOM Institute AMOLF, Science Park 104, 1098 XE Amsterdam, The Netherlands*

(Dated: August 24, 2022)

Making copies of information-carrying polymers is a defining feature of living systems. A true, “persistent” copy is a high free-energy state with template and copy sequence-correlated but non-interacting. We identify a general measure of the thermodynamic efficiency with which this high free-energy state is created, and analyze the copy accuracy and efficiency of a family of dynamical models that produce persistent copies. For the weakest chemical driving, when polymer growth occurs in equilibrium, both the copy accuracy and, more surprisingly, the efficiency vanish. At higher driving strengths, accuracy and efficiency both increase, with efficiency showing one or more peaks at moderate driving. Correlations generated within the copy sequence, as well as between template and copy, store additional free energy in the copied polymer and limit the single-site accuracy for a given chemical work input. Our results provide insight in the design of natural self-replicating systems and can aid the design of man-made replicators.

The copying of information from a template into a substrate is fundamental to life. The most powerful copying mechanisms are persistent, autonomous and generic. A persistent copy retains the copied data after physically decoupling from its template [7, 8]. An autonomous copy process does not require systematically time-varying external conditions [8], making it more versatile. Finally, a generic copy process is able to copy arbitrary data. DNA replication and both steps of gene expression necessarily exhibit all three characteristics.

Unlike natural systems, synthetic copying mechanisms developed hitherto have not incorporated all three features. Early work focused on using template polymers to synthesize specific daughter polymers, but failed to adequately demonstrate subsequent separation of copy and template [9, 10]. We describe such a process as templated self-assembly (TSA), by analogy with structures that assemble with high specificity due to favourable contacts in the final state.

Due to cooperativity, the tendency of copies to remain bound to templates grows with template length [11–13]. Consequently, generic copying of long polymers (as opposed to dimers and trimers [11, 14, 15]) has proved challenging. One tactic is to consider environments in which the system experiences cyclically varying conditions, with assembly of the copy favoured in one set of conditions and detachment from the template in another [16–18]. A more subtle approach is to use a spatially non-uniform environment, so that individual molecules undergo cyclic variation in conditions [19]. Whilst these experiments may indeed reflect early life [20, 21], they do not demonstrate copying in a truly autonomous context.

We also contrast the copying of a generic polymer sequence with the approach in Refs. [13, 22]. Here, the information is propagated between successive units of a single self-assembling polymer, rather than between a template and a daughter polymer, limiting information transmission. Externally induced mechanical stress on

long length scales severs the polymers, leading to more nucleation sites and exponential growth.

These challenges suggest that a full understanding of the basic biophysics of copying is lacking. Previous theoretical work on polymer copying mechanisms [1–6, 23] has addressed TSA, ignoring persistence. Recently, Ref. [7] outlined thermodynamic constraints imposed on copying by persistence, but without exploring autonomous mechanisms.

In this work we analyze a family of model systems that generate persistent copies in an autonomous and generic way. We introduce a new metric for the thermodynamic efficiency of copying, and investigate the accuracy and efficiency of our models. We highlight the profound consequences of requiring persistence, with both the copy accuracy and efficiency vanishing close to equilibrium. We further find that intra-copy-sequence correlations arise naturally. These correlations store additional free energy in the copied polymer, which do not contribute towards the accuracy of copying.

## MODELS AND METHODS

### Model definition

We consider a copy polymer  $M = M_1, \dots, M_L$ , made up of a series of sub-units or monomers  $M_x$ , growing with respect to a template  $N = N_1, \dots, N_L$  ( $l \leq L$ ). Inspired by transcription and translation, we consider a copy that detaches from the template as it grows; fig. 1b shows the simplest model of this type. We consider whole steps in which a single monomer is added or removed, encompassing many individual chemical sub-steps [1, 2]. After each step there is only a single inter-polymer bond at position  $l$ , between  $M_l$  and  $N_l$ . As a new monomer joins the copy at position  $l + 1$ , the bond position  $l$  is broken, contrasting with previous models of TSA [1–6] (Fig. 1a).

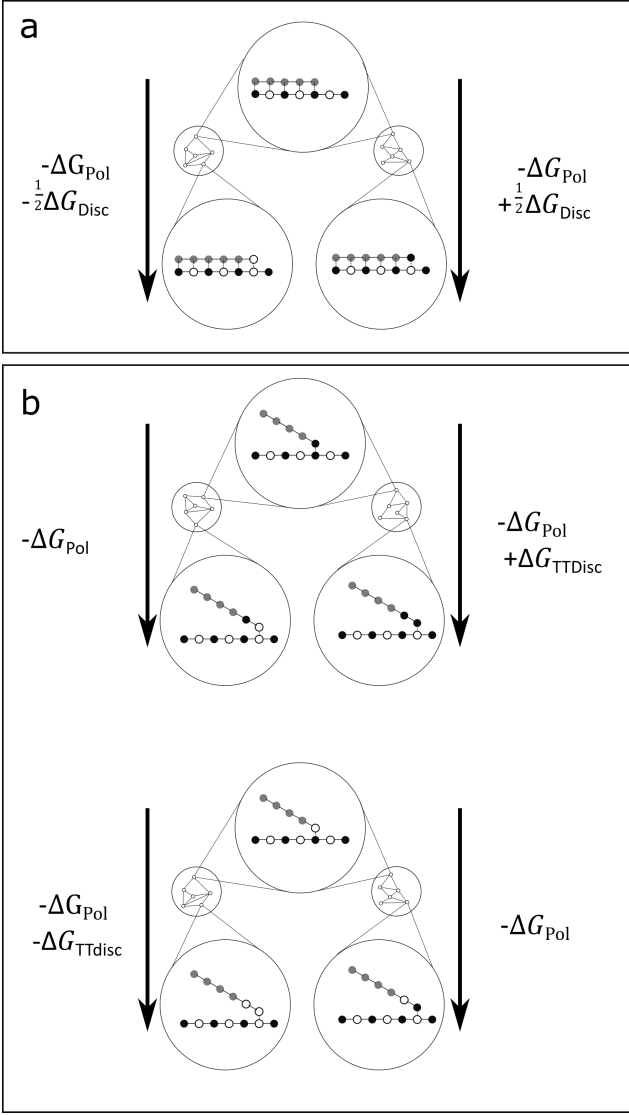


FIG. 1. Simple mechanisms for (a) templated self-assembly and (b) the creation of persistent polymer copies. Each of the diagrams, when viewed from top to bottom, describe the complete addition of a single monomer to a growing polymer chain, with the addition of a correct monomer on the left hand branch and an incorrect monomer on the right hand branch. Implicit intermediate states and individual chemical reactions are illustrated schematically within the small circles [1, 2]. In simple models of non-persistent copying [1–6] the overall free-energy change for addition is determined solely by knowledge of the added monomer. In a simple mechanism that produces persistent copies, the bond between the penultimate monomer in the copy and the template must break as the next monomer is added. Consequently, the free energy change now depends on both of these two leading monomers. This breaking of bonds means that no overall thermodynamic bias for correct matches between copy and template can survive in the long term, and generates non-trivial correlations within the copy sequence.

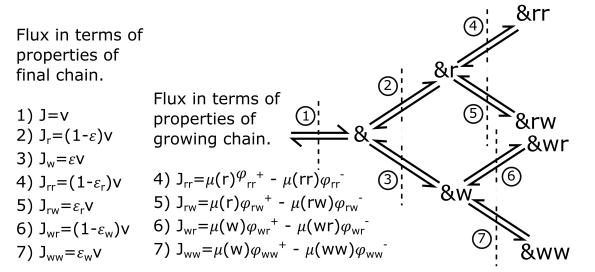


FIG. 2. Transitions of an arbitrary polymer  $\&$ . To relate the final chain to the growing chain it is useful to consider fluxes through interfaces in this transition diagram. Using the tip and combined probabilities, along with relative propensities it is possible to describe the fluxes through interfaces 4–7 in terms of properties of the growing chain. Equally by considering errors and conditional errors and taking fractions of the overall growth velocity, it is possible to find the fluxes through interfaces 4–7 in terms of properties of the final chain and growth velocity.

Importantly, as explained below, each step now depends on both of the two leading monomers, generating extra correlations within the copy sequence.

Following earlier work, we assume that both polymers are copolymers, and that the two monomer types are symmetric [1–6]. Thus the relevant question is whether monomers  $M_l$  and  $N_l$  match; we therefore ignore the specific sequence of  $N$  and describe  $M_l$  simply as right or wrong. Thus  $M_l \in r, w$ ; with example chain  $M = rrwrrrrrrwrr$ . An excess of  $r$  indicates a correlation between template and copy sequences. Breaking this symmetry would favour specific template sequences over others, disfavouring the accurate copying of other templates and compromising the generality of the process.

Given the model’s state space, we now consider state free energies (which must be time-invariant for autonomy). We treat the environment as a bath of monomers at constant chemical potential [1–6]. By symmetry, extending the polymer while leaving the copy-template interaction unchanged involves a fixed polymerization free energy. We thus define  $-\Delta G_{\text{pol}}$  as the chemical free-energy change for the transition between any specific sequence  $m_1, \dots, m_l$  and any specific sequence  $m_1, \dots, m_{l+1}$ , ignoring any contribution from interactions with the template. We then define  $\Delta G_{\text{TTDisc}}$  as the free-energy difference between  $r$  and  $w$  interactions with template. This bias is “temporary” as it only lasts until that contact is broken.

Overall, each forward step makes and breaks one copy-template bond. There are four possibilities: either adding  $r$  or  $w$  at position  $l+1$  to a template with  $M_l = r$ ; or adding  $r$  or  $w$  in position  $l+1$  to a template with  $M_l = w$ . The first and last of these options make and break the same kind of template bond, so the total free-energy change is  $-\Delta G_{\text{pol}}$ . For the second case there is a  $r$  bond broken and a  $w$  bond added, implying a free-energy change of  $-\Delta G_{\text{pol}} + \Delta G_{\text{TTDisc}}$ . Conversely, for the third

case, there is a  $w$  bond broken and a  $r$  bond added, giving a free-energy change of  $-\Delta G_{\text{pol}} - \Delta G_{\text{TDisC}}$ . These constraints are shown in fig. 1b; they fundamentally differentiate our model from TSA (fig. 1a).

Having specified model thermodynamics, we now parameterize kinetics. We assume that there are no “futile cycles”, such as appear in kinetic proofreading [24, 25]. Each step thus requires a well defined input of free energy determined by  $-\Delta G_{\text{pol}}$  and  $\pm \Delta G_{\text{TDisC}}$  [26], and no free-energy release occurs without a step. Reactions are tightly coupled, and the polymer state specifies the reaction history.

A full kinetic treatment would be a continuous time Markov process incorporating the intermediate states shown schematically in fig. 1b. To identify sequence output, however, we need only consider the state space in fig. 1b and the relative probabilities for transitions between these explicitly modelled states, ignoring the complexity of non-exponential transition waiting times [1]. We define propensities  $\psi_{xy}^+$  as the rate per unit time in which a system in state  $\&x$  starts the process of becoming  $\&xy$  and  $\psi_{xy}^-$  as the equivalent quantity in the reverse direction ( $\&$  is an unspecified polymer sequence). Our system has eight of these propensities ( $\psi_{rr}^\pm$ ,  $\psi_{rw}^\pm$ ,  $\psi_{wr}^\pm$  and  $\psi_{ww}^\pm$ ); the simplest TSA models require four [1–3, 5, 6].

The free-energy changes for each pair of forward and backwards transitions fix the ratios  $\psi_{xy}^+/\psi_{xy}^-$ . For simplicity we assume that the propensity for adding  $r$  is independent of the previous monomer:  $\psi_{rr}^+ = \psi_{wr}^+$ . Similarly  $\psi_{rw}^+ = \psi_{ww}^+ = 1$ , also defining the overall timescale. Only the ratio  $\psi_{xr}^+/\psi_{xw}^+$  remains unspecified; we parameterise it via  $\psi_{xr}^+/\psi_{xw}^+ = \Delta G_{\text{Kdisc}}/k_B T$  by analogy with transition state theory. Introducing  $\Delta G_{\text{Kdisc}}$  allows the study of systems where  $r$  is “kinetically” favoured [2, 3].  $\Delta G_{\text{TDisC}} > 0$  describes systems with temporary thermodynamic biases towards  $r$ , the closest analog of the “energetic case” in ref. [2]. Setting  $k_B T = 1$ ,

$$\psi_{rr}^+ = e^{\Delta G_{\text{Kdisc}}}, \psi_{rr}^- = e^{-\Delta G_{\text{pol}}} e^{\Delta G_{\text{Kdisc}}}, \quad (1)$$

$$\psi_{rw}^+ = 1, \psi_{rw}^- = e^{-\Delta G_{\text{pol}}} e^{\Delta G_{\text{TDisC}}}, \quad (2)$$

$$\psi_{wr}^+ = e^{\Delta G_{\text{Kdisc}}}, \psi_{wr}^- = e^{-\Delta G_{\text{pol}}} e^{\Delta G_{\text{Kdisc}}} e^{-\Delta G_{\text{TDisC}}}, \quad (3)$$

$$\psi_{ww}^+ = 1, \psi_{ww}^- = e^{-\Delta G_{\text{pol}}}. \quad (4)$$

For a given  $\Delta G_{\text{Kdisc}}$ ,  $\Delta G_{\text{pol}}$  and  $\Delta G_{\text{TDisC}}$ , eqs. 1-4 describe a set of models with distinct intermediate states that all produce the same copy sequence distribution. To study this distribution we analyze the simplest model in each set, in which the process is Markovian at the level of the explicitly modelled states and  $\psi_{xy}^\pm$  are rate constants.

### Model analysis.

We use Gaspard’s method to solve for copy sequence growth [23]. In this approach, the tip-monomer identity probabilities ( $\mu(m_l)$ ), the joint tip and penultimate monomer identity probabilities ( $\mu(m_{l-1}, m_l)$ ), and the

conditional probabilities ( $\mu(m_{l-1}|m_l)$ ) become stationary for a long polymer and can be calculated. One must first calculate the partial velocities,  $v_r$  and  $v_w$ . The quantity  $v_x \mu(x)$  is the net rate at which monomers are added after an  $x$ ,

$$v_x = \psi_{xr}^+ - \frac{\mu(x|r)\mu(r)}{\mu(x)} \psi_{xr}^- + \psi_{xw}^+ - \frac{\mu(x|w)\mu(w)}{\mu(x)} \psi_{xw}^-. \quad (5)$$

Following ref. [23], these velocities can be rewritten as

$$v_x = \frac{\psi_{xr}^+ v_r}{\psi_{xr}^- + v_r} + \frac{\psi_{xw}^+ v_w}{\psi_{xw}^- + v_w}. \quad (6)$$

Allowing  $x = r, w$  gives a pair of simultaneous equations that can be solved exactly, but inelegantly. We therefore proceed numerically and obtain tip and conditional probabilities via

$$\mu(x) = \frac{\psi_{rx}^+}{\psi_{rx}^- + v_x} \mu(r) + \frac{\psi_{wx}^+}{\psi_{wx}^- + v_x} \mu(w), \quad (7)$$

$$\mu(x|y) = \frac{\psi_{xy}^+}{\psi_{xy}^- + v_y} \mu(y). \quad (8)$$

Gaspard’s method describes the tips of growing chains. We, however, require the eventual result after the tip has moved on, the “final” monomer at site  $n$ :  $M_n^\infty$ . As discussed in the supplementary material,  $M_n^\infty$  can have very different properties from  $M_n$  near the tip.  $M_n^\infty$  is described by the error probability  $\epsilon$  and the conditional error probabilities  $\epsilon_r$  and  $\epsilon_w$ , defined as the probability that  $M_{n+1}^\infty = w$  given that  $M_n^\infty = r$  or  $M_n^\infty = w$ , respectively. We show that  $\epsilon$ ,  $\epsilon_r$  and  $\epsilon_w$  are sufficient in the supplementary material, by proving that the  $M^\infty$  is a Markov chain of  $r$  and  $w$  monomers (this requirement is distinct from the Markovian growth dynamics). We note that  $\epsilon \neq \epsilon_r \neq \epsilon_w$  as a direct result of the dependence of the transition propensities on the current and previous tip monomers, which in turn arises from detachment.

To calculate  $\epsilon$ ,  $\epsilon_r$  and  $\epsilon_w$ , we define currents  $J_{xy}$  that are related to both  $\psi_{xy}^\pm$  and  $\epsilon$ ,  $\epsilon_r$  and  $\epsilon_w$  separately. The current  $J_{xy}$  is the net rate per unit time at which transitions  $\&x \rightarrow \&xy$  occur:  $J_{xy} = \psi_{xy}^+ \mu(x) - \psi_{xy}^- \mu(x, y)$ . By considering the transitions in our system as a tree, as in Fig. 2, we can relate the current through a branch to the overall rate at which errors are permanently incorporated into a polymer growing at total velocity  $v = v_r \mu(r) + v_w \mu(w)$ .

$$J_{rr} = (1 - \epsilon)(1 - \epsilon_r)v = \mu(r)\psi_{rr}^+ - \mu(r, r)\psi_{rr}^-, \quad (9)$$

$$J_{rw} = (1 - \epsilon)\epsilon_r v = \mu(r)\psi_{rw}^+ - \mu(r, w)\psi_{rw}^-, \quad (10)$$

$$J_{wr} = \epsilon(1 - \epsilon_w)v = \mu(w)\psi_{wr}^+ - \mu(w, r)\psi_{wr}^-, \quad (11)$$

$$J_{ww} = \epsilon\epsilon_w v = \mu(w)\psi_{ww}^+ - \mu(w, w)\psi_{ww}^-. \quad (12)$$

Solving these simultaneous equations allows us to calculate the two conditional errors,  $\epsilon_r$  and  $\epsilon_w$ . To find  $\epsilon$

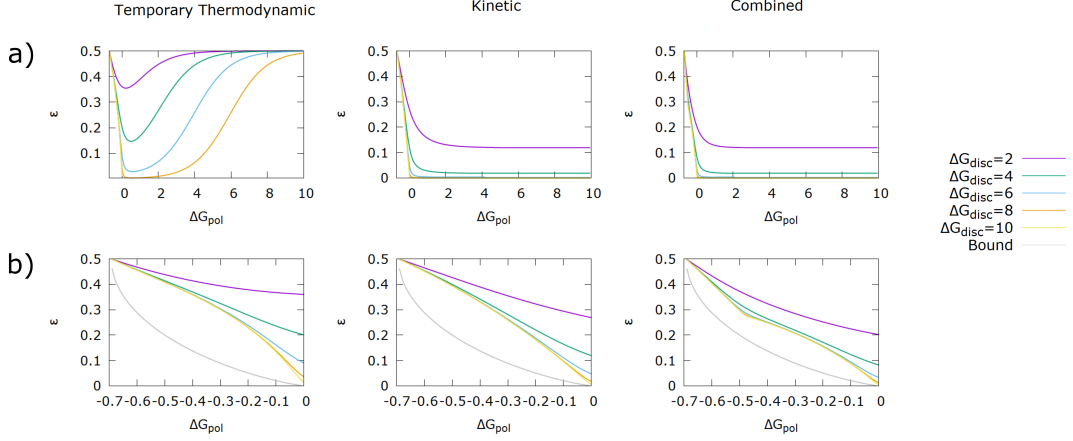


FIG. 3. Error probability  $\epsilon$  as a function of  $\Delta G_{\text{pol}}$  for all three mechanisms: (a) over a wide range of  $\Delta G_{\text{pol}}$ , and (b) within the entropy-driven region  $\Delta G_{\text{pol}} \leq 0$ . The temporary thermodynamic mechanism is always least accurate, and the combined mechanism most accurate. All mechanisms have no accuracy in the limit of  $\epsilon \rightarrow 0$ , and are far from the fundamental bound on single-site accuracy imposed by  $H_{ss} = -\epsilon \ln \epsilon - (1 - \epsilon) \ln(1 - \epsilon) \geq -\Delta G_{\text{pol}}$  except at  $\Delta G_{\text{pol}} \approx 0$ .

we exploit the fact that the final sequence has a transition matrix parameterised by  $\epsilon_r$  and  $\epsilon_w$ , with the overall error  $\epsilon$  given by this matrix's dominant eigenvector. As detailed in the supplementary information, we obtain  $\epsilon = \epsilon_r / (1 + \epsilon_r - \epsilon_w)$ . From  $\epsilon$ ,  $\epsilon_r$  and  $\epsilon_w$  we calculate properties of the copy in terms of  $\psi_{xy}^\pm$  and thus the free energies. We corroborate the analytical results with simulation (see supplementary material).

## RESULTS

### General thermodynamic bounds

The free energy of the combined bath and polymer system decreases over time. There are two contributions to the free-energy change per added monomer: the chemical free energy  $\Delta G_{\text{pol}}$ , and a contribution from the uncertainty of the final polymer sequence [7]. The latter is quantified by the entropy rate  $H$  [27, 28]:

$$H(M^\infty) = \lim_{n \rightarrow \infty} \frac{1}{n} H(M_1^\infty, M_2^\infty, \dots, M_n^\infty), \quad (13)$$

which in our case is given by [28]

$$H(M^\infty) = -\epsilon (\epsilon_w \ln \epsilon_w + (1 - \epsilon_w) \ln(1 - \epsilon_w)) - (1 - \epsilon) (\epsilon_r \ln \epsilon_r + (1 - \epsilon_r) \ln(1 - \epsilon_r)). \quad (14)$$

The overall free energy change per added monomer is then  $\Delta G_{\text{tot}} = -\Delta G_{\text{pol}} - H$ , which must be negative for growth:  $H \geq -\Delta G_{\text{pol}}$ . Since copy-template interactions are not extensive in the copy length, they do not contribute. Given that  $H \geq 0$ , growth is possible in the

region where  $\Delta G_{\text{pol}} < 0$ , corresponding to the “entropically driven” regime [3, 6].

The entropy rate is bounded by the single site entropy  $H \leq H_{ss} = -\epsilon \ln \epsilon - (1 - \epsilon) \ln(1 - \epsilon)$ .  $H_{ss}$  quantifies the desired correlations *between* copy and template. For previous models of TSA with uncorrelated monomer incorporation,  $H = H_{ss}$  [1–6, 23]. In our model, the necessary complexity of  $\psi_{xy}^\pm$  generates correlations *within* the copy. A stronger constraint on the single site entropy, and hence accuracy, then follows:  $H_{ss} \geq H \geq -\Delta G_{\text{pol}}$ .

Fundamentally, a persistent copy is a high free energy state, as the entropic cost of copy-template correlations cannot be counteracted by stabilizing copy-template interactions. Thus the process moves a system between two high free energy states, converting chemical work into correlations. While in some cases all of the chemical work done by the monomer bath is retained in the final state, with no dissipation, this is not generally the case and so it is natural to introduce an efficiency. The overall free energy stored in the polymer has contributions from both the creation of an equilibrium (uncorrelated) polymer and contributions above this due to correlations both within the copy and with the template. We are interested only in the contributions above equilibrium. The efficiency  $\eta$  is then the proportion of the additional free energy expended in making a copy above the minimum required to grow a random equilibrium polymer that is successfully converted into the non-equilibrium free energy of the copy sequence rather than being dissipated. In our simple case,

$$\eta \equiv \frac{H_{\text{eq}} - H}{H_{\text{eq}} + \Delta G_{\text{pol}}} \leq 1. \quad (15)$$

Here,  $\Delta G_{\text{pol}} + H_{\text{eq}} = \Delta G_{\text{pol}} + \ln 2$  is the extra chemical work done by the buffer above that required to grow an



equilibrium polymer,  $\Delta G_{\text{pol}}^{\text{eq}} = -H_{\text{eq}} = -\ln 2$ . The free energy stored in the copy sequence, above that stored in an equilibrium system, is  $H_{\text{eq}} - H$ .  $\eta \leq 1$  follows from  $\Delta G_{\text{pol}} + H \geq 0$ . Similarly, since  $H_{\text{ss}} \leq H$  we can define a single-site efficiency

$$\eta_{\text{ss}} \equiv \frac{H_{\text{eq}} - H_{\text{ss}}}{H_{\text{eq}} + \Delta G_{\text{pol}}} \leq \eta \leq 1. \quad (16)$$

Unlike  $\eta$ , the single site efficiency  $\eta_{\text{ss}}$  discounts the free energy stored in “useless” correlations *within* the copy.

### Behaviour of specific systems

We consider three representative discrimination mechanisms consistent with eqs. 1-4. Firstly, for comparison, we use the kinetic discrimination mechanism proposed by Bennett for TSA [3], in which  $r$  and  $w$  bind equally strongly to the template, but  $r$  monomers are added and removed more quickly. This mechanism is coincidentally a special case of persistent copying since there is no permanent thermodynamic bias, and is obtained by setting  $\Delta G_{\text{TTdisc}} = 0$  and  $\Delta G_{\text{Kdisc}} = \Delta G_{\text{disc}}$  in equations 1-4.

We then introduce two new mechanisms. “Temporary thermodynamic discrimination” includes a difference in template binding strengths for  $r$  and  $w$ , while keeping addition rates equal. The need for persistence renders any thermodynamic advantage of  $r$  temporary, unlike in TSA [5]. In this case we set  $\Delta G_{\text{Kdisc}} = 0$  and  $\Delta G_{\text{TTdisc}} = \Delta G_{\text{disc}}$ . Finally, we consider a “combined discrimination mechanism” with equal kinetic and temporary thermodynamic discrimination, in which both template binding strengths and rates of addition favour  $r$  monomers. For this approach we set  $\Delta G_{\text{Kdisc}} = \Delta G_{\text{TTdisc}} = \Delta G_{\text{disc}}$ .

All three mechanisms have two free parameters, the overall driving strength  $\Delta G_{\text{pol}}$  and the discrimination parameter  $\Delta G$ . We plot error probability against  $\Delta G_{\text{pol}}$  for various  $\Delta G_{\text{disc}}$  in fig. 3. Also shown is the thermodynamic lower bound on  $\epsilon$  implied by  $H_{\text{ss}} \geq H \geq -\Delta G_{\text{pol}}$ . All three cases have no accuracy ( $\epsilon = 0.5$ ) as  $\Delta G_{\text{pol}} \rightarrow -\ln 2$ , the limit of equilibrium growth. This result is expected, since an accurate persistent copy is necessarily out of equilibrium [7]. By contrast, TSA allows for accuracy in equilibrium [2, 5, 29].

The temporary thermodynamic mechanism is always the least effective. It has no accuracy for high  $\Delta G_{\text{pol}}$  as the difference between  $r$  and  $w$  is only manifest when stepping backwards, and for high  $\Delta G_{\text{pol}}$  back steps are rare [2, 5]. More interestingly, temporary thermodynamic discrimination is also inaccurate as  $\Delta G_{\text{pol}} \rightarrow -\ln 2$ , when the system takes so many back steps that it fully equilibrates. Low  $\epsilon$  only occurs when  $\Delta G_{\text{pol}}$  is sufficient to inhibit the detachment of  $r$  monomers, but not the detachment of  $w$  monomers. This trade-off region grows with  $\Delta G_{\text{disc}}$ . By contrast, both the combined case and the kinetic case have accuracy in the limit of  $\Delta G_{\text{pol}} \rightarrow \infty$ , since they allow  $r$  to bind faster than  $w$ .

Considering  $\Delta G_{\text{pol}} \leq 0$  closely (fig. 3b) shows the combined case to be the superior of the two.

Intriguingly, all three mechanisms are far from the fundamental bound on  $\epsilon$  implied by  $H_{\text{ss}} \geq H \geq -\Delta G_{\text{pol}}$  as  $\Delta G_{\text{pol}} \rightarrow -\ln 2$ , and there is an apparent cusp in  $\epsilon$  at  $\Delta G_{\text{pol}} \approx 0.48$  as  $\Delta G_{\text{disc}} \rightarrow \infty$  in the combined case. The performance relative to the bound is quantified by  $\eta_{\text{ss}}$  (fig. 4). Surprisingly, we observe in fig. 4a that not only does  $\epsilon$  go to zero as  $\Delta G_{\text{pol}} \rightarrow -\ln 2$ , so does  $\eta_{\text{ss}}$  in all cases. For small non-equilibrium driving, none of the extra chemical work input is stored in correlations with the template. Mathematically, this inefficiency arises because  $\epsilon - 0.5 \propto \Delta G_{\text{pol}} - \ln 2$  as  $\Delta G_{\text{pol}} \rightarrow -\ln 2$  (as observed in fig. 3), and  $H_{\text{ss}} - \ln 2 \propto (\epsilon - 0.5)^2$  for  $\epsilon \approx 0.5$  by definition. Thus, from equation 16,  $\eta_{\text{ss}} \propto \Delta G_{\text{pol}} - \ln 2$  as  $\Delta G_{\text{pol}} \rightarrow -\ln 2$ . That this result only depends on error probability decreasing proportionally with  $\Delta G_{\text{pol}}$  for small driving suggests that a vanishing  $\eta_{\text{ss}}$  in equilibrium may be quite general.

In all cases, the single-site efficiency  $\eta_{\text{ss}}$  increases from 0 at  $\Delta G_{\text{pol}} = -\ln 2$  to a peak near  $\Delta G_{\text{pol}} = 0$ , with  $\eta_{\text{ss}} \rightarrow 1$  as  $\Delta G_{\text{disc}} \rightarrow \infty$ . Beyond this peak,  $\eta_{\text{ss}}$  tends to zero since the stored free energy is bounded by  $\ln 2$  per monomer. To understand the peak, note that for every  $\Delta G_{\text{pol}} \leq 0$  there is a hypothetical highest accuracy copy with  $\epsilon$  fixed by  $H_{\text{ss}} = -\Delta G_{\text{pol}}$  that is marginally thermodynamically permitted. However, this copy is not generally kinetically accessible. At  $\Delta G_{\text{pol}} = 0$  the marginal copy is the completely accurate one. Unlike at lower values of  $\Delta G_{\text{pol}}$ , however, all three mechanisms’ kinetics allow us to get close to this particular marginal copy, resulting in a peak. This peak tends to unity as  $\Delta G_{\text{disc}} \rightarrow \infty$  but approaches this limit even for moderate values of  $\Delta G_{\text{disc}}$ . We note that as  $\Delta G_{\text{disc}} \rightarrow \infty$ , growth is slow for all  $\Delta G_{\text{pol}} \leq 0$ , in that the total number of steps taken diverges.

A related argument explains the apparent cusp in the error  $\epsilon$  for the combined mechanism at  $\Delta G_{\text{pol}} \approx -0.48$  and high  $\Delta G_{\text{disc}}$ . On the plot of  $\eta_{\text{ss}}$  (fig. 4a) this cusp manifests as a shoulder. For the full efficiency  $\eta$  (fig. 4b), we see a prominent second peak. Uniquely, the combined mechanism’s kinetics strongly disfavour chains of consecutive  $w$ s for high  $\Delta G_{\text{disc}}$ . A final copy with no consecutive  $w$ s has  $\epsilon_w = 0$  but  $\epsilon_r \neq 0$ . Maximizing the entropy rate of such a Markov chain over  $\epsilon_r$  gives  $H_{\text{max}} = 0.48121$ ;  $\Delta G_{\text{pol}} = -H_{\text{max}}$  matches the location of our peak/cusp. Thus the combined mechanism initially eliminates consecutive  $w$ s, and at  $\Delta G_{\text{pol}} = -0.48121$  a state with  $\eta_w = 0$  is thermodynamically permitted for the first time. For large  $\Delta G_{\text{disc}}$ , this polymer is kinetically accessible and grows with thermodynamic efficiency approaching unity (fig. 4c). In this limit, the overall entropy generation is zero.

The above behaviour is a striking example of correlations being generated within the copy sequence, as well as with the template. Notably, whilst  $\eta$  approaches unity at this point,  $\eta_{\text{ss}}$  does not (fig. 4). Correlations *within* the copy sequence limit the chemical work that

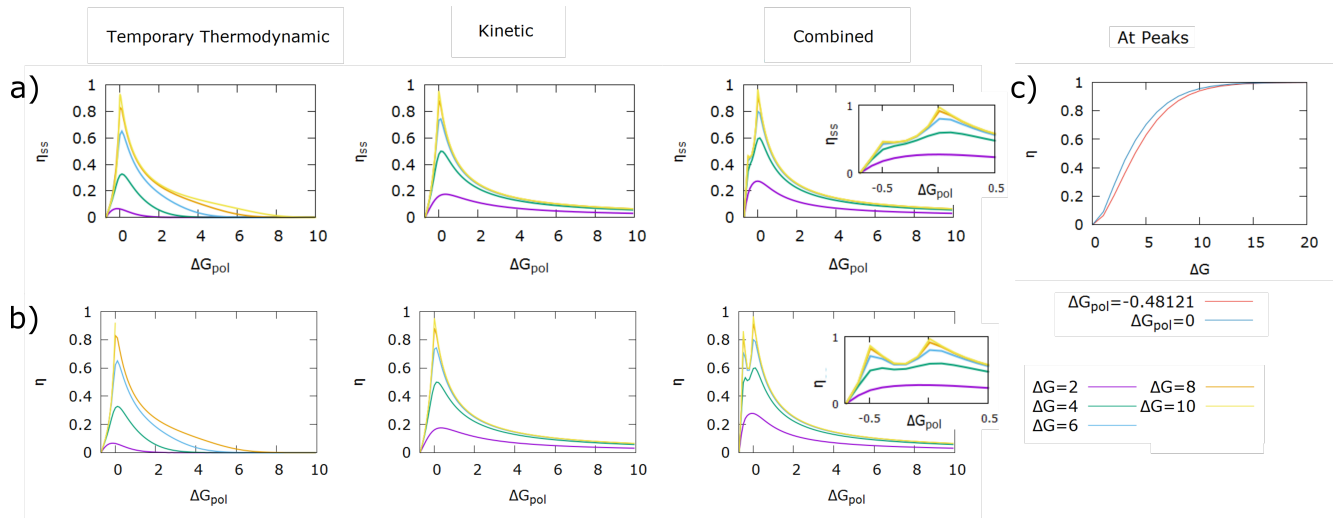


FIG. 4. Efficiencies  $\eta_{ss}$  (a) and  $\eta$  (b) plotted against  $\Delta G_{pol}$  show sharp peaks at  $\Delta G_{pol} = 0$  as  $\Delta G_{disc} \rightarrow \infty$  in all three cases. In the combined case we see a second peak in  $\eta$ , and a shoulder in  $\eta_{ss}$  at  $\Delta G_{pol} = -0.48121$ . (c) Both of these peaks in  $\eta$  tend to unity at  $\Delta G_{disc} \rightarrow \infty$ .

can be devoted to improving the single site accuracy of the copy polymer, since they prevent the bound  $H_{ss} \geq H \geq -\Delta G_{pol}$  from being saturated.

## CONCLUSION

The thermodynamic constraint on copying is deceptively simple: overall, the chemical contribution to the free-energy of a copy is independent of the match between template and copy sequences. By studying the simplest mechanisms satisfying this constraint, however, we can draw important conclusions for copying mechanisms and thermodynamics more generally.

For copying mechanisms, the most immediate contrast with previous work on TSA [1–6, 23] is that accuracy is necessarily zero when the copy assembles in equilibrium, since it is impossible to have equilibrium correlations between physically separated polymers [7]. Consequently, unlike self-assembly, no autonomous copying system can rely on relaxation to near-equilibrium; fundamentally different paradigms are required.

Further, we find that solely relying on correct monomers binding more strongly to the template is ineffective when creating non-equilibrium persistent copies. At  $\Delta G_{disc} = 6k_B T$ , a cost comparable to a single mismatched base pair [30], the temporary thermodynamic discrimination model never improves upon  $\epsilon = 0.0285$ , which is more than ten times the equilibrium error probability based on energetic discrimination obtainable in TSA,  $1/(1 + \exp(\Delta G_{disc}))$ . This performance would degrade further if multiple competing incorrect monomers were present. We therefore predict that some degree of “kinetic” discrimination is vital for any persistent copying mechanism. Such kinetic discrimination must arise

from the details of the microscopic sub-steps that are implicit in this work; putative enzyme-free replicators should be highly optimized in this regard. We are currently exploring which behaviours arise naturally in simple models with explicit sub-steps.

Correlations within the copy, as well as between copy and template, arise naturally in persistent mechanisms. Indeed, in one of our models, pairs of mistakes are eliminated well before individual mistakes. These correlations contribute to the non-equilibrium free energy of the final state, detracting from the single-site copy accuracy achievable for a given chemical work input. However, in biology it is arguably the accuracy of whole sequences, rather than individual monomers, that matters. In this case, positive correlations could advantageously increase the number of completely correct copies for a given average error rate. It remains to be seen whether this tactic is feasible. Either way, we predict that correlations during copying may be significant, particularly in simple systems with only moderate accuracy. These correlations may change significantly if the requirement to remain bound with one exactly bond is relaxed, and exploiting correlations to extend functionality beyond simple copying is an intriguing prospect.

Thermodynamically, a persistent copying mechanism converts the high free energy of the input molecules into a high free-energy copy state; we have defined a general efficiency of this free-energy transduction for copying. In typical physical systems with tight coupling of reactions, high efficiency occurs when the load is closely matched to the driving, either in autonomous systems operating near the stall force, or in quasistatically manipulated systems. For the polymer copying mechanisms studied here, however, we find that the thermodynamic efficiency of information transfer, and not just the accuracy, approaches

zero as polymer growth stalls. We predict that this result is general, since the alternative would require a sub-linear convergence of the error rate on 50% as thermodynamic driving tends towards the stall point.

Fundamentally, the copy process transduces free energy into a complex system with many degrees of freedom (the sequence), and not just the polymer length. To be accurate, the sequence must be prevented from equilibrating. Thus, whilst weak driving leads to polymer growth with little overall entropy generation, it does a poor job of pushing the polymer sequence out of equilibrium. We predict that similar behaviour will arise in other systems intended to create an output in which a subset of the degrees of freedom are out of equilibrium.

Away from the equilibrium limit, the efficiency shows one or more peaks as the polymerization free energy is varied. At these peaks, the system transitions between two non-equilibrium states with remarkably little dissipation. These particular values of  $\Delta G_{\text{pol}}$  are sufficient to stabilise non-equilibrium distributions that happen to be especially kinetically accessible, rendering the true equilibrium particularly inaccessible. This alignment of kinetic and thermodynamic factors is most evident in the combined mechanism that efficiently produces a state with few adjacent mismatches at  $\Delta G_{\text{pol}} = -0.48121$ . These results slightly qualify the prediction of Ref. [7] that accurate copying is necessarily entropy generating, since entropy generation can be made arbitrarily small, whilst retaining finite copy accuracy, by taking

$\Delta G_{\text{disc}} \rightarrow \infty$  at these specific values of  $\Delta G_{\text{pol}}$ .

The behaviour of the efficiency in these models emphasizes the importance, in both natural and synthetic copying systems, of kinetically preventing equilibration. Our work emphasizes that this paradigm should be applied not only to highly-evolved systems with kinetic proofreading mechanisms [24, 25], but also the most basic mechanisms imaginable.

Extending our analysis to consider kinetic proofreading cycles would be natural. It is well-established that kinetic proofreading can enhance discrimination in thermodynamic models of TSA for a given intrinsic  $\Delta G_{\text{disc}}$  [2, 3, 31]; the same is likely true for copying, although in this case one cannot simply rely on enhancing an equilibrium bias. Indeed, the limited returns available from temporary thermodynamic discrimination may make kinetic proofreading even more important for persistent copies, given that  $\Delta G_{\text{disc}}$  is constrained by underlying chemistry. The entropy of the copy sequence will still be thermodynamically constrained:  $H_{\text{ss}} \geq H \geq -\Delta G_{\text{pol}} - \Delta G_{\text{fuel}}$ , where the final term is the additional free energy expended per step to drive the system around proofreading cycles. We predict that non-equilibrium proofreading cycles, by their very nature, are unlikely to approach efficiencies of unity.

We are grateful to Charles Bennett for instructive conversations. TEO is supported by the Royal Society and PRtW is supported by the Netherlands Organisation for Scientific Research (NWO).

- 
- [1] Cady F, Qian H (2009) Open-system thermodynamic analysis of DNA polymerase fidelity. *PHYS BIOL* 6:036011.
  - [2] Sartori P, Pigolotti S (2015) Thermodynamics of error correction. *PHYS REV X* 5:041039.
  - [3] Bennett CH (1979) Dissipation-error tradeoff in proofreading. *BIOSYSTEMS* 11:85–91.
  - [4] Andrieux D, Gaspard P (2008) Nonequilibrium generation of information in copolymerization processes. *PROC NAT ACAD SCI USA* 105:9516–9521.
  - [5] Sartori P, Pigolotti S (2013) Kinetic versus energetic discrimination in biological copying. *PHYS REV LETT* 110:188101.
  - [6] Esposito M, Lindenberg K, Van den Broeck C (2010) Extracting chemical energy by growing disorder: efficiency at maximum power. *J STAT MECH-THEORY E* 2010:P01008.
  - [7] Ouldridge TE, ten Wolde PR (2017) Fundamental costs in the production and destruction of persistent polymer copies. *PHYS REV LETT* 118:158103.
  - [8] Ouldridge TE, Govern CC, ten Wolde PR (2017) Thermodynamics of computational copying in biochemical systems. *Phys. Rev. X* 7:021004.
  - [9] Tjivikua T, Ballester P, Rebek Jr J (1990) Self-replicating system. *J AMM PHYS SOC* 112:1249–1250.
  - [10] Feng Q, Park TK, Rebek J (1992) Crossover reactions between synthetic replicators yield active and inactive recombinants. *SCIENCE* 256:1179–1180.
  - [11] Vidonne A, Philp D (2009) Making molecules make themselves—the chemistry of artificial replicators. *EUR J ORG CHEM* 2009:593–610.
  - [12] Orgel LE (1992) Molecular replication. *NATURE* 358:203.
  - [13] Colomb-Delsuc M, Mattia E, Sadownik JW, Otto S (2015) Exponential self-replication enabled through a fibre elongation/breakage mechanism. *NAT COMMUN* 6:7427.
  - [14] Sievers D, Von Kiedrowski G (1994) Self-replication of complementary nucleotide-based oligomers. *NATURE* 369:221–224.
  - [15] Lincoln TA, Joyce GF (2009) Self-sustained replication of an RNA enzyme. *SCIENCE* 323:1229–1232.
  - [16] Wu N, Willner I (2016) ph-stimulated reconfiguration and structural isomerization of origami dimer and trimer systems. *NANO LETT* 16:6650–6655.
  - [17] Wang T, et al. (2011) Self-replication of information-bearing nanoscale patterns. *NATURE* 478:225–228.
  - [18] Li T, Nicolaou K (1994) Chemical self-replication of palindromic duplex dna. *NATURE* 369:218–221.
  - [19] Mast CB, Braun D (2010) Thermal trap for DNA replication. *PHYS REV LETT* 104:188102.
  - [20] Orgel LE (1998) The origin of lifea review of facts and speculations. *TRENDS BIOCHEM SCI* 23:491–495.
  - [21] Martin W, Baross J, Kelley D, Russell MJ (2008) Hy-

- drothermal vents and the origin of life. *NAT REV MICROBIOL* 6:805.
- [22] Schulman R, Yurke B, Winfree E (2012) Robust self-replication of combinatorial information via crystal growth and scission. *PROC NAT ACAD SCI USA* 109:6405–6410.
- [23] Gaspard P, Andrieux D (2014) Kinetics and thermodynamics of first-order markov chain copolymerization. *J CHEM PHYS* 141:044908.
- [24] Hopfield JJ (1974) Kinetic proofreading: A new mechanism for reducing errors in biosynthetic processes requiring high specificity. *PROC NAT ACAD SCI USA* 71:4135–4139.
- [25] Ninio J (1975) Kinetic amplification of enzyme discrimination. *BIOCHIMIE* 57:587–595.
- [26] Esposito M (2018) Thermodynamically consistent coarse graining of biocatalysts beyond michaelis-menten. *B AM PHYS SOC*.
- [27] Boyd AB, Mandal D, Crutchfield JP (2016) Identifying functional thermodynamics in autonomous maxwellian ratchets. *NEW J PHYS* 18:023049.
- [28] Cover TM, Thomas JA (2012) *Elements of information theory*. (John Wiley & Sons).
- [29] Johansson M, Lovmar M, Ehrenberg M (2008) Rate and accuracy of bacterial protein synthesis revisited. *CURR OPIN MICROBIOL* 11:141–147.
- [30] John SantaLucia J, Hicks D (2004) The thermodynamics of DNA structural motifs. *Annu. Rev. Biophys. and Biomol. Struct.* 33:415–440.
- [31] Ehrenberg M, Blomberg C (1980) Thermodynamic constraints on kinetic proofreading in biosynthetic pathways. *BIOPHYS J* 31:333 – 358.
- [32] Gillespie DT (1977) Exact stochastic simulation of coupled chemical reactions. *J CHEM PHYS* 81:2340–2361.

## SUPPORTING INFORMATION (SI)

### Difference between the tip probabilities and the final sequence

It might not be immediately obvious why the properties of the growing chain described by  $\mu(m_l)$  and  $\mu(m_l, m_{l-1})$  should be different from those of the final chain described by  $\epsilon$ ,  $\epsilon_r$  and  $\epsilon_w$ , but the difference can be illustrated with a simple example. Consider a system in which incorrect monomers could be added to the end of the chain, but where nothing can be added after an incorrect match. In this case while the tip probability for an incorrect match  $\mu(w)$  would be finite, the error of the final chain  $\epsilon$  would be vanishingly small, as all incorrect matches would have to be removed in order for the polymer to grow further.

### Demonstrating that the sequence of the final chain is Markovian

Let  $M_n^\infty$  be the monomer at the  $n$ th site in the final chain. Let a polymer be represented by  $M_1^\infty, \dots, M_n^\infty$ . The probability of a given chain existing is then

$P^\infty(m_1, \dots, m_n)$ . In order for the sequence of monomers moving along the chain (increasing  $n$ ) to be able to be represented by a Markov chain, the condition

$$P^\infty(m_n | m_{n-1}, \dots, m_1) = P^\infty(m_n | m_{n-1}) \quad (17)$$

must hold.

In order to demonstrate that eq. 17 holds, we rewrite the final chain probability in terms of properties of the growing chain. Specifically we state that the probability of the sequence  $m_1, \dots, m_n$  existing in the final chain is the product of the probability  $Q(m_1, \dots, m_{n-1}, t)$  that the chain is in the state  $m_1, \dots, m_{n-1}$  at a time  $t$  during the growth process, and the propensity  $\nu(m_n; m_1, \dots, m_{n-1})$  with which  $m_n$  is added to a chain  $m_1, \dots, m_{n-1}$  and never removed, integrated over all time. It should be noted that  $r(m_n; m_1, \dots, m_{n-1})$  is time-independent.

$$P^\infty(m_1, \dots, m_n) = \int Q(m_1, \dots, m_{n-1}, t) \nu(m_n; m_1, \dots, m_{n-1}) dt \quad (18)$$

$$P^\infty(m_1, \dots, m_n) = \nu(m_n; m_1, \dots, m_{n-1}) \int Q(m_1, \dots, m_{n-1}, t) dt \quad (19)$$

Setting the integral equal to  $I(m_1, \dots, m_{n-1})$  gives

$$P^\infty(m_1, \dots, m_n) = \nu(m_n; m_1, \dots, m_{n-1}) I(m_1, \dots, m_{n-1}) \quad (20)$$

Let's consider the probabilities of two sub-sequences, identical except for the final monomer. We call the two final monomers  $m_n$  and  $m'_n$  and we can denote the ratios of the probabilities of these two chains as follows.

$$\frac{P^\infty(m_1, \dots, m_n)}{P^\infty(m_1, \dots, m'_n)} = \frac{\nu(m_n; m_1, \dots, m_{n-1}) I(m_1, \dots, m_{n-1})}{\nu(m'_n; m_1, \dots, m_{n-1}) I(m_1, \dots, m_{n-1})} \quad (21)$$

The  $I$  terms are independent of this final monomer and so cancel. Thus

$$\frac{P^\infty(m_1, \dots, m_n)}{P^\infty(m_1, \dots, m'_n)} = \frac{\nu(m_n; m_1, \dots, m_{n-1})}{\nu(m'_n; m_1, \dots, m_{n-1})} \quad (22)$$

The same relationship holds for the conditional probabilities

$$\frac{P^\infty(m_n | m_1, \dots, m_{n-1})}{P^\infty(m'_n | m_1, \dots, m_{n-1})} = \frac{r(m_n; m_1, \dots, m_{n-1})}{r(m'_n; m_1, \dots, m_{n-1})} \quad (23)$$

For our system, the propensity with which a monomer  $m_n$  is added and never removed,  $\nu(m_n; m_1, \dots, m_{n-1})$ , is dependent on only on the final two monomers in the sequence fragment,  $m_n$  and  $m_{n-1}$ . To see why, note that this propensity is determined by addition and removal of monomers at sites  $i \geq n$ . The identities of monomers at positions  $j < n - 1$ , however, only influence addition and removal propensities at sites  $k < n$  (eq. 1-4). Thus we convert  $\nu(m_n; m_1, \dots, m_{n-1})$  to  $f(m_n, m_{n-1})$ .

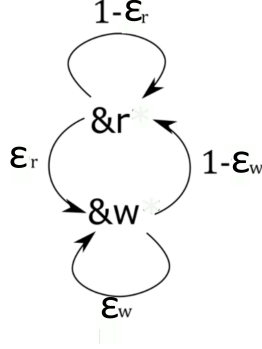


FIG. 5. The transition diagram for the Markov process describing the sequence of monomers found by stepping forward along a completed chain.

$$\frac{P^\infty(m_n|m_1, \dots, m_{n-1})}{P^\infty(m'_n|m_1, \dots, m_{n-1})} = \frac{f(m_n, m_{n-1})}{f(m'_n, m_{n-1})} \quad (24)$$

Multiplying both sides by  $P^\infty(m_1, \dots, m_{n-2})$  and summing over all values of  $m_1, \dots, m_{n-2}$  (recall  $\sum_{c,d} P(a|b, c, d)P(c, d) = P(a|b)$  and  $\sum_{c,d} P(c, d) = 1$ ) gives

$$\frac{P(m_n|m_{n-1})}{P(m'_n|m_{n-1})} = \frac{f(m_n, m_{n-1})}{f(m'_n, m_{n-1})}. \quad (25)$$

Comparing equations 24 and 25 yields:

$$\frac{P^\infty(m_n|m_{n-1}, \dots, m_1)}{P(m'_n|m_{n-1}, \dots, m_1)} = \frac{P^\infty(m_n|m_{n-1})}{P^\infty(m'_n|m_{n-1})}. \quad (26)$$

Summing over the possible values of  $m'_n$  and recalling that  $P^\infty(r|m_{n-1}) + P^\infty(w|m_{n-1}) = 1$  and

$P^\infty(r|m_{n-1}, \dots, m_1) + P^\infty(w|m_{n-1}, \dots, m_1) = 1$  yields:

$$P^\infty(m_n|m_{n-1}, \dots, m_1) = P^\infty(m_n|m_{n-1}), \quad (27)$$

thereby proving that the sequence of the final chain is Markovian.

#### Overall error probability of the final chain

The final sequence is described by the Markov chain illustrated in figure 5. The transition matrix for this process is

$$T = \begin{bmatrix} 1 - \epsilon_r & 1 - \epsilon_w \\ \epsilon_r & \epsilon_w \end{bmatrix}, \quad (28)$$

The eigenvector of this transition matrix with eigenvalue equal to unity gives the steady state of the Markov chain. The second component of this eigenvector corresponds to the overall probability of incorrect matches,  $\epsilon$ :

$$\epsilon = \epsilon_r / (1 + \epsilon_r - \epsilon_w). \quad (29)$$

#### Corroboration with simulation

To check the analytical methods used to solve the system we also simulated the growth of a polymer. We used a Gillespie simulation [32], with transition rates given by  $\psi_{xy}^\pm$ . Simulations were initialised with a randomly determined two monomer sequence, and truncated as soon as the polymer reached 1000 monomers. We found that such a length rendered edge effects negligible in all but the most extreme cases for the calculation of  $\epsilon$ . Polymer error probabilities were inferred directly from the 100 simulations, and are compared to analytical results in fig. 6.

We note in passing that the calculation of  $H$ ,  $H_{ss}$ , and particularly the efficiency's  $\eta$  and  $\eta_{ss}$ , are more vulnerable to random fluctuations in a simulation of finite length, and peculiar edge effects, than  $\epsilon$ . Gaspard's solution is therefore invaluable in reaching robust conclusions for these quantities.

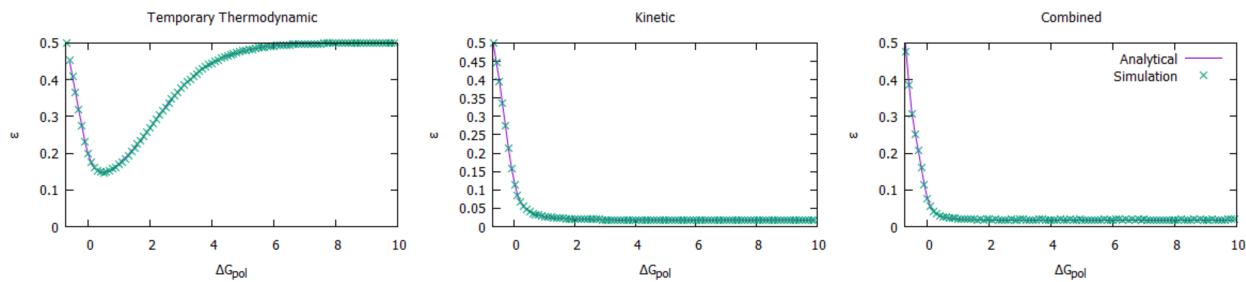


FIG. 6. Errors obtained from Gillespie simulations are indistinguishable from the analytical results obtained using Gaspard's method for all three mechanisms.